Orclever Proceedings of Research and Development
https://doi.org/10.56038/oprd.v4i1.456
OR CLEVER Science & Research Group

Conference Article

Performance Analysis of PID and Fuzzy Logic Controlled Semi-Active and Passive Suspension Elements on Full Vehicle Model

Umut Yaşar ESEN*,Muzaffer METİN[2]

[1] AVL Türkiye Research & Engineering, Istanbul, Türkiye, Orcid ID: https://orcid.org/0009-0007-7410-0441, E-mail: Umut.Esen@avl.com, yasar.esen@std.yildiz.edu.tr
[2] Faculty of Mechanical Engineering, Yildiz Technical University, Besiktas, Istanbul, Turkey , Orcid ID: https://orcid.org/0000-0002-9724-3433, E-mail: mmetin@yildiz.edu.tr
* Correspondence: yasar.esen@std.yildiz.edu.tr; Tel.: (+90505456284)

4th International Conference on Access to Recent Advances in Engineering and Digitalization
May 27 - 28, 2024

Received 10 February 2024
Received in revised form 18 May 2024
In final form 23 May 2024

Reference: Ersoy, P., Erşahin, M. Benchmarking Llama 3 70B for Code Generation: A Comprehensive Evaluation. Orclever Proceedings of Research and Development, 4(1), 59-72.

Abstract

In this study, the dynamic performances of full vehicle models were extensively investigated through simulations conducted in the MATLAB-Simulink environment to evaluate their responses to various system inputs, especially passive suspension elements and models equipped with semi-active Magneto-Rheological (MR) dampers. Initially, a full vehicle model was created using passive suspension elements, and the system behaviors against different road inputs are analyzed. Subsequently, integration of a semi-active MR damper onto the same full vehicle model is performed, and this specific damper was controlled using two different control methods: the first control method is selected as PID, and the second one as a Fuzzy Logic Controller (FLC). The system's responses to various road inputs are examined for both control methods and the respective controllers. This study stands out as a method used in the design and performance analysis of suspension systems for full-vehicle models. The results, especially regarding the control of semi-active MR dampers with a Fuzzy Logic Controller, indicate that semi-active dampers can respond more effectively to different road conditions and enhance ride comfort.

Keywords: *Vehicle vibrations, MR damper, Semi-active control, Vehicle dynamics, Full vehicle, Fuzzy Logic Controller, PID Controller,*

https://doi.org/10.56038/oprd.v4i1.456

1. Introduction

The complex interplay between vehicles and road conditions, marked by variations in surface roughness and resulting vibrations, constitutes a crucial aspect influencing both human well-being and the overall comfort of transportation. As such, the effectiveness of vehicle suspension systems emerges as a pivotal factor in managing and mitigating these dynamic forces. Suspension systems, fundamental components of automotive engineering, are typically categorized into three primary variants: passive, active, and semi-active. While passive suspension systems are favored for their straightforward design and widespread adoption, they often face limitations in adequately attenuating vibrations compared to their more sophisticated counterparts [2]. This highlights the ongoing pursuit of automotive innovation to develop advanced suspension technologies capable of providing enhanced ride quality and minimizing the adverse effects of road-induced vibrations on passenger comfort and vehicle performance. Such advancements not only contribute to safer and more comfortable transportation experiences but also underscore the relentless pursuit of excellence within the automotive industry in addressing evolving challenges in mobility and human well-being.

This study focuses on evaluating the dynamic performance of full-vehicle models by investigating models equipped with both passive suspension elements and semi-active MR dampers. Utilizing MATLAB-Simulink simulations, the research first analyzes the behavior of a vehicle model with passive suspension. Subsequently, it integrates a semi-active MR damper into the same model. Furthermore, two distinct control methods are employed to regulate the MR damper, and the performance of these controllers is assessed across various system inputs. Specifically, both PID and Fuzzy Logic controllers are utilized for MR damper control in this study. The findings of this research showcase that the semi-active MR damper exhibits more efficient responses under different road conditions and control methods, thus potentially enhancing overall ride comfort. Through its comprehensive analysis, this study holds the promise of significantly contributing to the design and performance evaluation of suspension systems for full-vehicle models, thereby advancing the field of automotive engineering.

https://doi.org/10.56038/oprd.v4i1.456

2. System Modelling

2.1. Physical Model

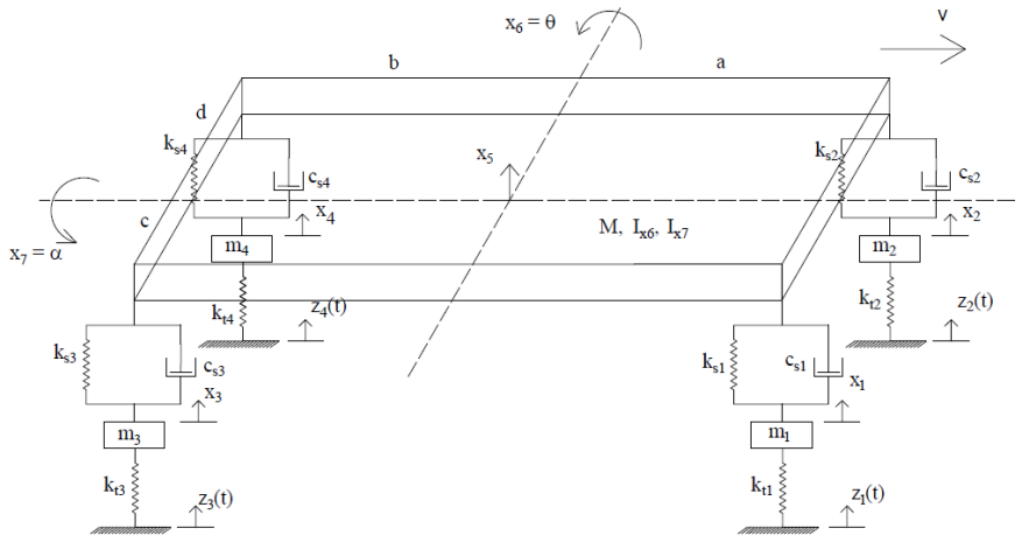

Figure 1: System Model

As seen in Figure 1, the wheel masses are denoted by m_1, m_2, m_3, m_4; wheel spring coefficients by k_{t_1}, k_{t_2}, k_{t_3}, k_{t_4}, the suspension spring coefficients by k_{s_1}, k_{s_2}, k_{s_3}, k_{s_4}, suspension damping coefficients by c_{s_1}, c_{s_2}, c_{s_3}, c_{s_4} vehicle mass by M, inertia moments about rotation axes by I_{x_6} and I_{x_7}, vertical motion of wheel masses by x_1, x_2, x_3, x_4, vertical motion of the body by x_5 at center of gravity (COG) point, pitch motion by $x_6 = \theta$, roll motion by $x_7 = \alpha$, and vehicle speed by V.

2.2. Mathematical Model

This study addresses a multi-degree-of-freedom system using the Lagrange method for mathematical modeling. The system is modeled using the energy-based approach of Lagrange formalism given by:

$$\frac{d}{dt}\left(\frac{\partial E_k}{\partial \dot{x}_j}\right) - \left(\frac{\partial E_k}{\partial x_j}\right) + \left(\frac{\partial E_p}{\partial x_j}\right) + \left(\frac{\partial E_D}{\partial \dot{x}_j}\right) = Q_j \quad (1)$$

https://doi.org/10.56038/oprd.v4i1.456

where E_k, E_p and E_D are kinetic energy, potential energy, damping energy respectively. For the equations of motion of the system using the Lagrange method, the total kinetic energy of the system is given as

$$E_k = \frac{1}{2}(M\dot{x}_5^2 + I_{x6}\dot{x}_6^2 + I_{x7}\dot{x}_7^2 + m_1\dot{x}_1^2 + m_2\dot{x}_2^2 + m_3\dot{x}_3^2 + m_4\dot{x}_4^2) \tag{2}$$

the total potential energy is

$$\begin{aligned} E_p = \frac{1}{2}(&k_{s1}(x_5 - x_1 + ax_6 - cx_7)^2 + k_{s2}(x_5 - x_2 + ax_6 + dx_7)^2 \\ &+k_{s3}(x_5 - x_3 - bx_6 - cx_7)^2 + k_{s4}(x_5 - x_4 - bx_6 + dx_7)^2 \\ &+k_{t1}(x_1 - z_1)^2 + k_{t2}(x_2 - z_2)^2 + k_{t3}(x_3 - z_3)^2 + k_{t4}(x_4 - z_4)^2) \end{aligned} \tag{3}$$

and the total damping energy is represented by

$$\begin{aligned} E_D = \frac{1}{2}(&c_{s1}(\dot{x}_5 - \dot{x}_1 + a\dot{x}_6 - c\dot{x}_7)^2 + c_{s2}(\dot{x}_5 - \dot{x}_2 + a\dot{x}_6 + d\dot{x}_7)^2 \\ &+c_{s3}(\dot{x}_5 - \dot{x}_3 - b\dot{x}_6 - c\dot{x}_7)^2 + c_{s4}(\dot{x}_5 - \dot{x}_4 - b\dot{x}_6 + d\dot{x}_7)^2) \end{aligned} \tag{4}$$

Then, the first equation of motion is derived as follows:

$$\begin{aligned} &(M\ddot{x}_5 + k_{s1}(x_5 - x_1 + ax_6 - cx_7) + k_{s2}(x_5 - x_2 + ax_6 + dx_7) \\ &+k_{s3}(x_5 - x_3 - bx_6 - cx_7) + k_{s4}(x_5 - x_4 - bx_6 + dx_7) \\ &+c_{s1}(\dot{x}_5 - \dot{x}_1 + a\dot{x}_6 - c\dot{x}_7) + c_{s2}(\dot{x}_5 - \dot{x}_2 + a\dot{x}_6 + d\dot{x}_7) \\ &+c_{s3}(\dot{x}_5 - \dot{x}_3 - b\dot{x}_6 - c\dot{x}_7) + c_{s4}(\dot{x}_5 - \dot{x}_4 - b\dot{x}_6 + d\dot{x}_7)) = 0 \end{aligned} \tag{5}$$

The second equation of motion is:

$$\begin{aligned} &(I_{x6}\ddot{x}_6 + k_{s1}a(x_5 - x_1 + ax_6 - cx_7) + k_{s2}a(x_5 - x_2 + ax_6 + dx_7) \\ &-k_{s3}b(x_5 - x_3 - bx_6 - cx_7) - k_{s4}b(x_5 - x_4 - bx_6 + dx_7) \\ &+c_{s1}a(\dot{x}_5 - \dot{x}_1 + a\dot{x}_6 - c\dot{x}_7) + c_{s2}a(\dot{x}_5 - \dot{x}_2 + a\dot{x}_6 + d\dot{x}_7) \\ &-c_{s3}b(\dot{x}_5 - \dot{x}_3 - b\dot{x}_6 - c\dot{x}_7) - c_{s4}b(\dot{x}_5 - \dot{x}_4 - b\dot{x}_6 + d\dot{x}_7)) = 0 \end{aligned} \tag{6}$$

https://doi.org/10.56038/oprd.v4i1.456

The third equation of motion is:

$$\begin{aligned}(I_{x7}\ddot{x}_7 - k_{s1}c(x_5 - x_1 + ax_6 - cx_7) + k_{s2}d(x_5 - x_2 + ax_6 + dx_7)\\ -k_{s3}c(x_5 - x_3 - bx_6 - cx_7) + k_{s4}d(x_5 - x_4 - ax_6 + dx_7)\\ -c_{s1}c(\dot{x}_5 - \dot{x}_1 + a\dot{x}_6 - c\dot{x}_7) + c_{s2}d(\dot{x}_5 - \dot{x}_2 + a\dot{x}_6 + d\dot{x}_7)\\ -c_{s3}c(\dot{x}_5 - \dot{x}_3 - b\dot{x}_6 - c\dot{x}_7) + c_{s4}d(\dot{x}_5 - \dot{x}_4 - a\dot{x}_6 + d\dot{x}_7)) = 0\end{aligned} \tag{7}$$

The fourth equation of motion is:

$$m_1\ddot{x}_1 - k_{s1}(x_5 - x_1 + ax_6 - cx_7) + k_{t1}(x_1 - z_1) - c_{s1}\left(\dot{x}_5 - \dot{x}_1 + a\dot{x}_6 - c\dot{x}_7\right) = 0 \tag{8}$$

The fifth equation of motion is:

$$m_2\ddot{x}_2 - k_{s2}(x_5 - x_2 + ax_6 + dx_7) + k_{t2}(x_2 - z_2) - c_{s2}\left(\dot{x}_5 - \dot{x}_2 + a\dot{x}_6 + d\dot{x}_7\right) = 0 \tag{9}$$

The sixth equation of motion is:

$$m_3\ddot{x}_3 - k_{s3}(x_5 - x_3 - bx_6 - cx_7) + k_{t3}(x_3 - z_3) - c_{s3}\left(\dot{x}_5 - \dot{x}_3 - b\dot{x}_6 - c\dot{x}_7\right) = 0 \tag{10}$$

The seventh equation of motion is:

$$m_4\ddot{x}_4 - k_{s4}(x_5 - x_4 - bx_6 + dx_7) + k_{t4}(x_4 - z_4) - c_{s4}\left(\dot{x}_5 - \dot{x}_4 - b\dot{x}_6 + d\dot{x}_7\right) = 0 \tag{11}$$

2.3. Magneto-Rheological (MR) Damper Model

In the literature, various models exist to successfully capture the damping force of MR dampers (such as the Bingham model, Bouc-Wen model, Lugre model, etc.). In this study, the Lugre model has been chosen for the mathematical modeling of the designed MR damper. The Lugre model is preferred due to its ability to achieve realistic results despite its simple structure [5]. Mathematically, the Lugre model is expressed as follows:

$$f = \sigma_a z + \sigma_0 z v + \sigma_1 \dot{z} + \sigma_2 \dot{x} + \sigma_b \dot{x} v \tag{12}$$

$$\dot{z} = \dot{x} - a_0|\dot{x}|z \tag{13}$$

https://doi.org/10.56038/oprd.v4i1.456

where f represents the damping force of the MR damper, $\dot{x}$ represents the relative velocity of the MR damper, v represents the voltage across the MR damper and z is the internal variable used to define the internal dynamics of the MR damper. $\Sigma_a, \sigma_0, \sigma_1, \sigma_2, \sigma_b$, and a_0 are the coefficients used to define the hysteresis character of the MR damper [4]. In line with this information, the system block diagram can be created as shown in Figure 2.

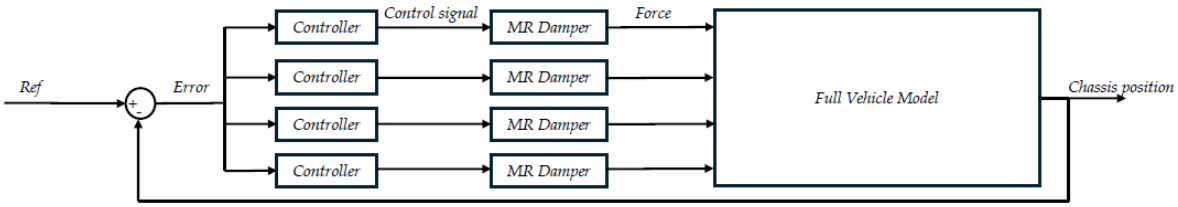

Figure 2: System Block Diagram

3. Controller Design

Various structural designs have been proposed in the realm of fuzzy PID controllers, encompassing PI and PD configurations. The conventional fuzzy PID controller (CFC) typically demands three inputs, thus resulting in a 3-dimensional rule base. However, the PID-type fuzzy controller operates with only two inputs, leading to a 2-dimensional rule base outperforming fuzzy PI and PD controllers. This superiority has been elaborately discussed in the design of a classical Fuzzy Controller. Within the scope of this study, an FLC was meticulously crafted utilizing MATLAB-Simulink and the Fuzzy Toolbox. The input variables of the FLC are elaborated upon in the Appendix section. Membership functions governing both scaled inputs (e, de) and the controller's output (u) are defined within the range of [-1, 1]. Triangular membership functions are selected for the error (Ke) and the derivative of error (Kde) input scaling factors, ensuring a 50% overlap. Standard triangular membership functions were chosen to augment the controller's efficacy. By leveraging these input and output membership functions, 15 rules were devised in the rule base. The centroid method was judiciously employed in this investigation for defuzzification [8]. The designed Fuzzy logic controller surface is as shown in Figure 3.

https://doi.org/10.56038/oprd.v4i1.456

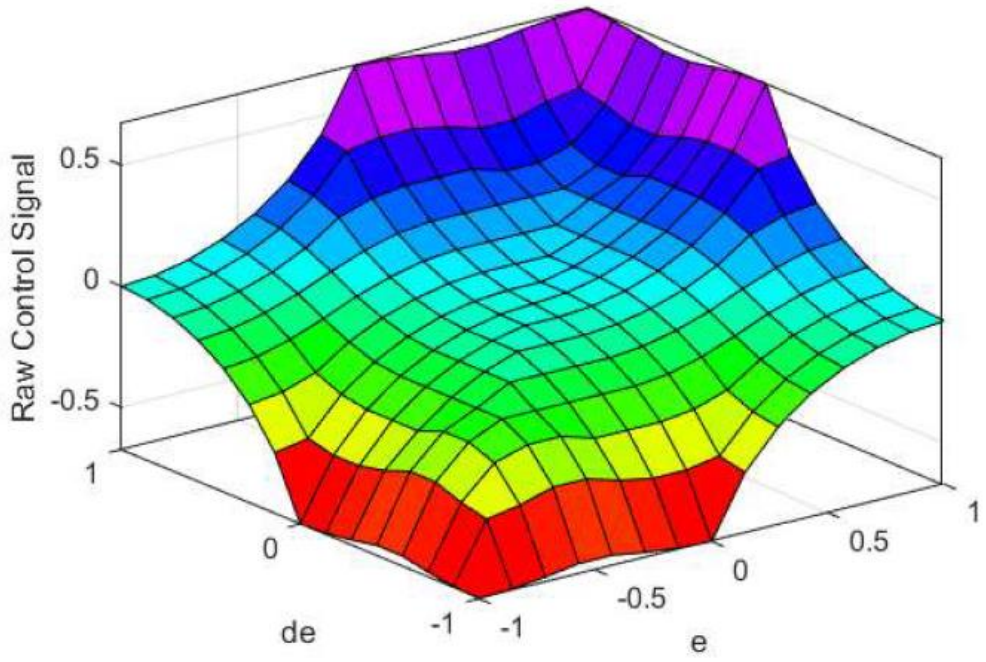

Figure 3: FLC Surface

The logic of creating the first controller is explained above. As the second method, a classical PID structure will be used to control the MR damper. Auto-tune in the MATLAB-Simulink program will be used to obtain classical PID coefficients.

4. Control and Simulation Application

This section explains the implementation of the mathematical model created in the MATLAB-Simulink environment and how to design controllers. Then, the simulation results for both the passive and semi-active systems will be obtained using MATLAB-Simulink. Here, a separate MR damper will be used for each wheel, just like in real life, and these MR dampers will be controlled using a PID and Fuzzy Logic Controller. Two different road disturbance inputs, each with a magnitude of 10 cm, will be applied to the system and the control performance is improved. The road disturbance inputs are given in Figure 4 and Figure 5.

https://doi.org/10.56038/oprd.v4i1.456

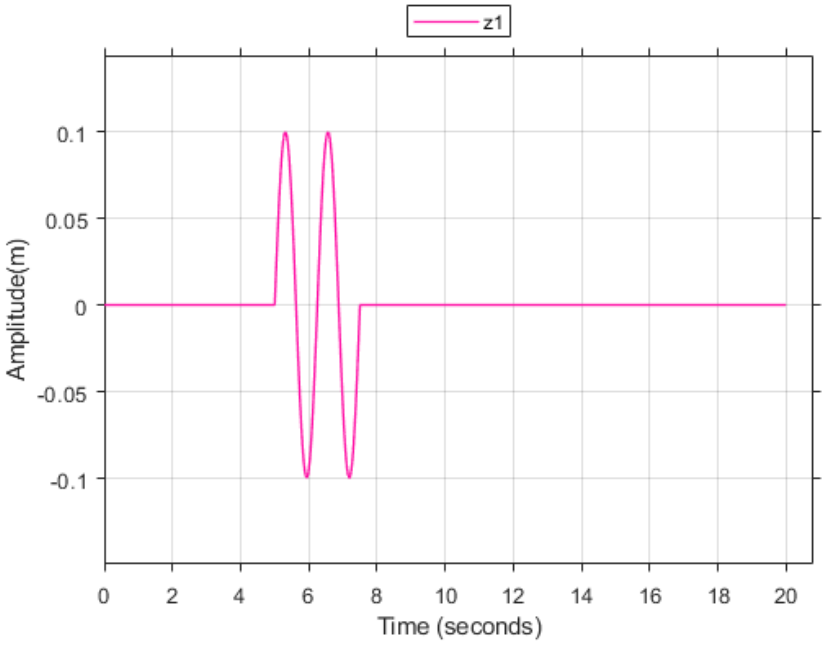

Figure 4: First Disturbance

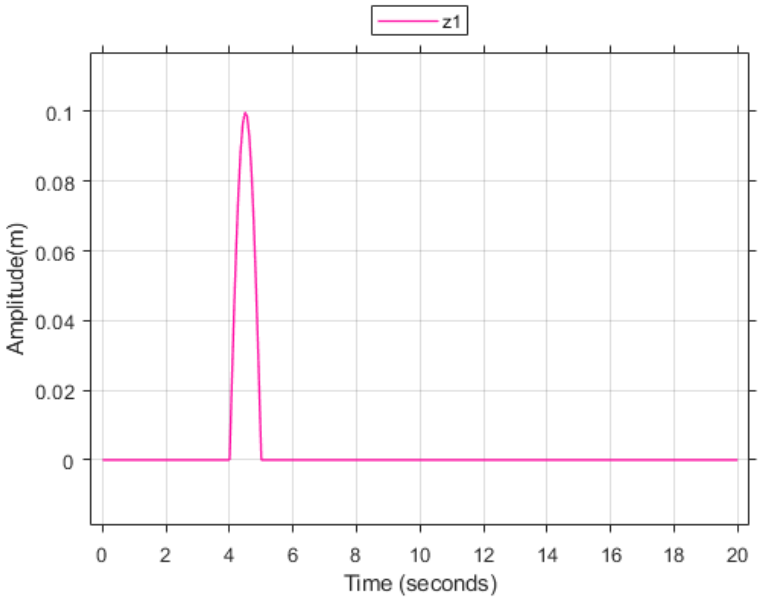

Figure 5: Second Disturbance

The disruptive inputs given above are applied to systems with both controllers separately and the system's responses are presented.

https://doi.org/10.56038/oprd.v4i1.456

5. Result

In this section, the simulation results obtained via MATLAB are provided, and the system responses of passive and semi-active suspensions are compared and discussed. (Note: '_PID' refers to the semi-active system controlled by the classical method PID. '_FLC' refers to the semi-active system controlled by Fuzzy PID. '_nocon' refers to the passive system.) One can refer to Section 2.1 for the correspondence of the vehicle statesx_5, x_6, and x_7. The system simulation results are shown in Figure 6, Figure 7, Figure 8 and Figure 9.

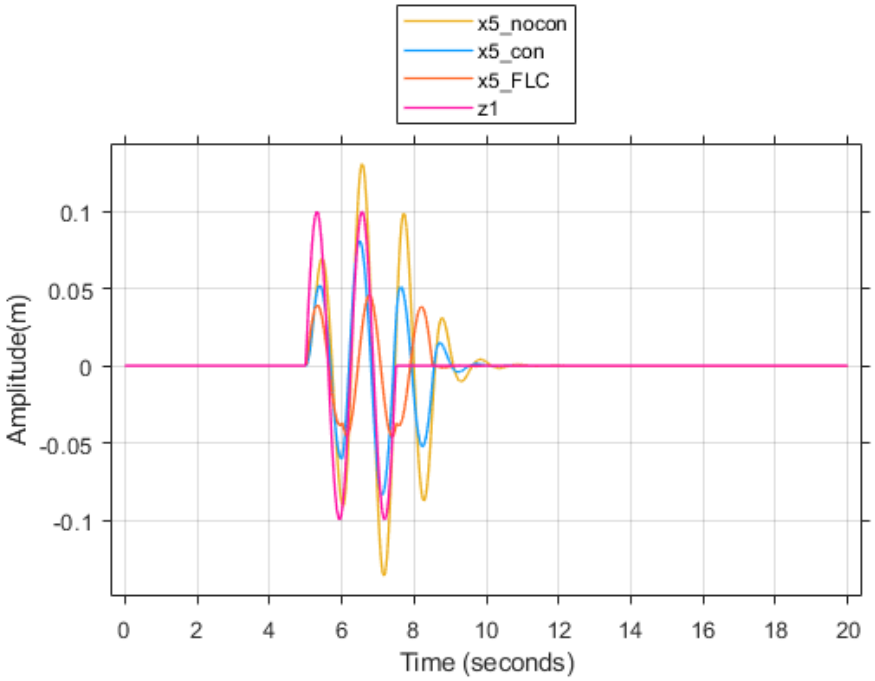

Figure 6: System Response for First Disturbance

https://doi.org/10.56038/oprd.v4i1.456

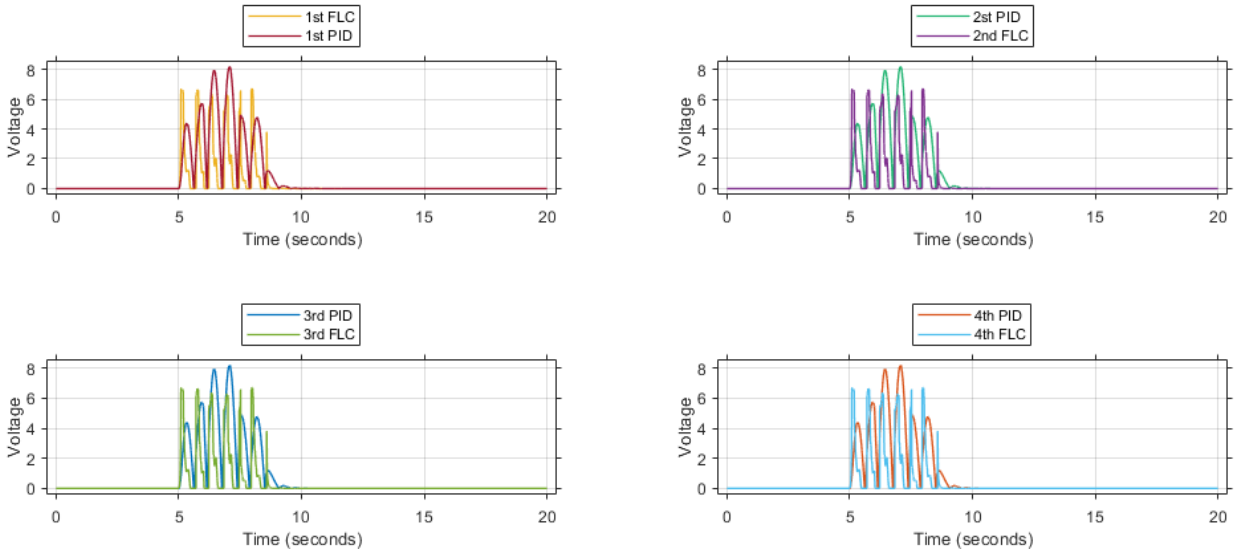

Figure 7: Control Signals for First Disturbance

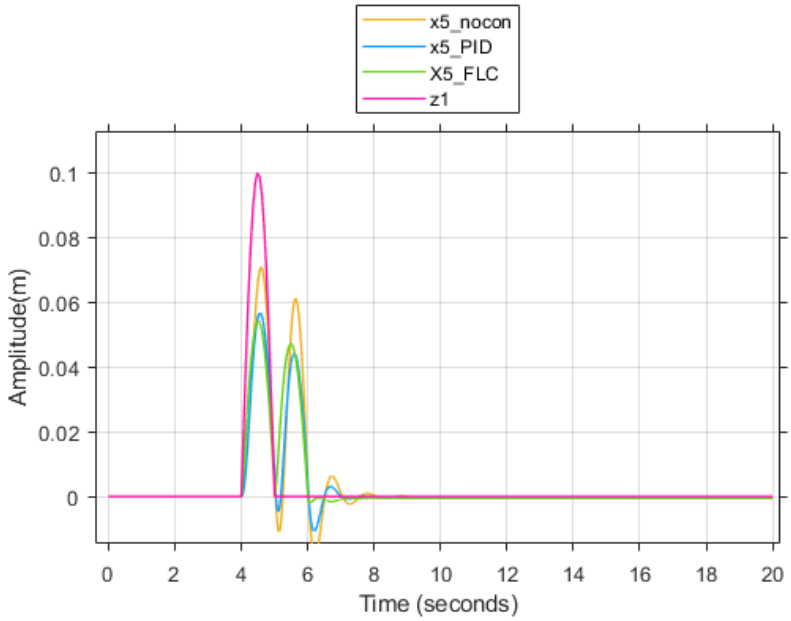

Figure 8: System Response for Second Disturbance

https://doi.org/10.56038/oprd.v4i1.456

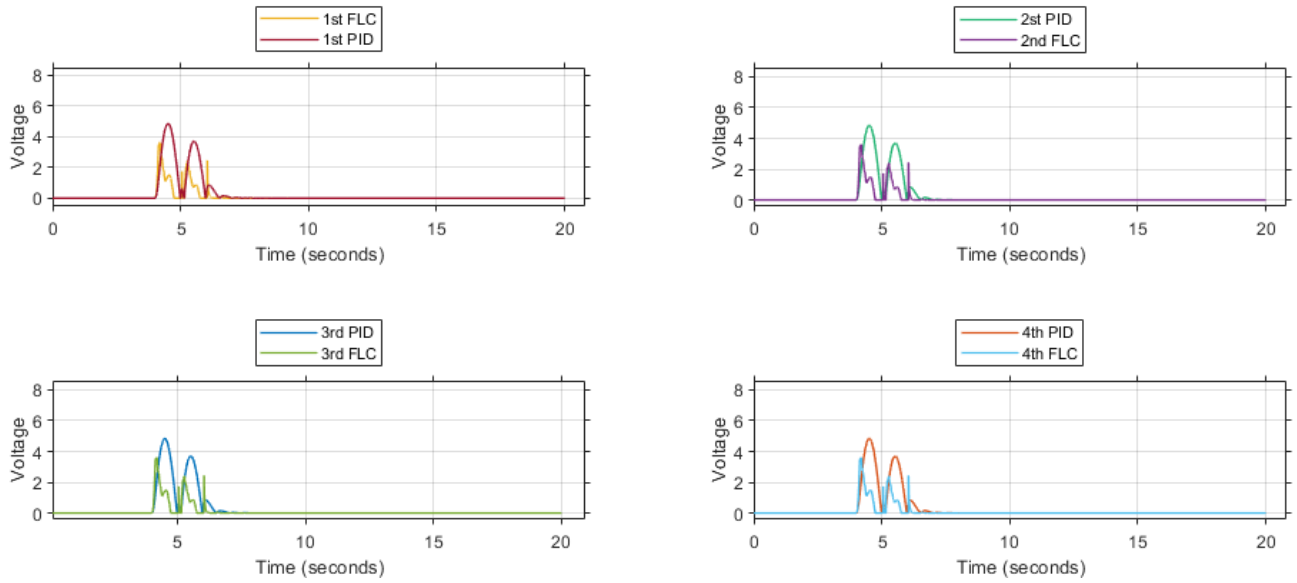

Figure 9: Control Signals for Second Disturbance

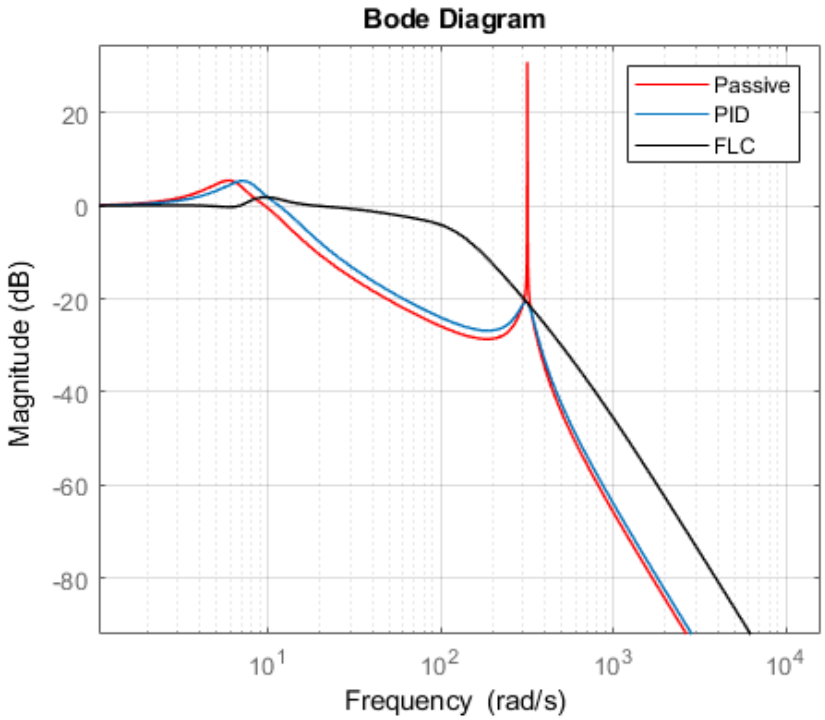

Figure 10: System Frequency Response

https://doi.org/10.56038/oprd.v4i1.456

From the Bode Diagram illustrated in Figure 10, it is observed that the FLC performs well in suppressing vibrations at low frequencies. The frequency of the disturbance signal in the time domain changes depending on the vehicle speed and the bumper length. Therefore, the range of variation in the disturbance signal frequency can be achieved based on the bumper length and vehicle speed. By looking at the upper limit of the frequency where the FLC is effective in the Bode diagram, it can be inferred that the FLC performs better for specific ranges of vehicle speed and bumper length. For all the considered road disturbance scenarios given above, the MR damper with FLC performs better than the passive suspension and the MR damper with PID control.

6. Discussion and Conclusion

This study focuses on integrating an MR damper into a full vehicle model with 7 degrees of freedom traveling at a constant speed of 10 km/h. The MR damper is controlled using two different methods, and their performances are compared with a passive suspension system. Upon scrutinizing the outcomes, the salutary impact of the MR damper on the system becomes apparent. Nevertheless, employing two distinct control methodologies on the MR damper reveals a convergence in their efficacy, as illustrated by the graphs. This convergence stems from both control methods driving the MR damper to a good performance. However, it is imperative to acknowledge that the primary variable under control is the vertical movement of the chassis. While not explicitly addressed here, the roll and pitch motions hold substantial significance for overall comfort. To maintain the study's focus, results concerning roll and pitch motions are omitted. Nonetheless, it can be inferred from undisclosed simulation outcomes that the system exhibits stability about the variables of vehicle roll and pitch angle.

Acknowledge

The first author acknowledges the valuable guidance and support of Dr. Baran Alikoç throughout the research. The authors also thank Yıldız Technical University, Institute of Science and Technology, for providing the necessary resources and facilities.

https://doi.org/10.56038/oprd.v4i1.456

References

[1] Abdi H, Valentin D, Edelman BE (1999). Neural networks. Sage, Thousand Oaks

[2] Abramowitz M, Stegun AI (1970) Handbook of mathematical function with formulas, graphs, and mathematical tables. Applied Mathematical Series, N.B.S.

[3] Agarwal M (1997) A systemic classification of neural-network-based control. IEEE Control Syst Mag 17, 2:75–93

[4] Agrawal A, Kulkarni P, Vieira SL, Naganathan NG (2001) An overview of magneto- and

[5] electro-rheological fluids and their applications in fluid power systems. Int J Fluid Power 2:5–36

[6] Ahmadian M, Marjoram RH (1989) Effects of passive and semi-active suspension on body and wheel-hop control. SAE paper 892487

[7] METİN, MUZAFFER and GÜÇLÜ, RAHMİ (2011) "Vibrations control of light rail transportation vehicle via PID type fuzzy controller using parameters adaptive method," Turkish Journal of Electrical Engineering and Computer Sciences: Vol. 19: No. 5, Article 11

[8] Al-Houlu N, Weaver J, Lahdhiri T, Joo DS (1999) Sliding mode-based fuzzy logic controller for a vehicle suspension system. American Control Conference, San Diego, USA, pp 4188–419

7. Appendix

Table 1: Parameters

Variables	Values	Unit	
m_1	25	kg	First wheel mass
m_2	25	kg	Second wheel mass
m_3	25	kg	Third wheel mass
m_4	25	kg	Fourth wheel mass
k_{t_1}	2500000	N/m	First wheel spring coefficient
k_{t_2}	2500000	N/m	Second wheel spring coefficient
k_{t_3}	2500000	N/m	Third wheel spring coefficient
k_{t_4}	2500000	N/m	Fourth wheel spring coefficient
k_{s_1}	15000	N/m	First suspension spring coefficient
k_{s_2}	15000	N/m	Second suspension spring coefficient
k_{s_3}	15000	N/m	Third suspension spring coefficient
k_{s_4}	15000	N/m	Fourth suspension spring coefficient
c_{s_1}	1250	Ns/m	First suspension damping coefficient

https://doi.org/10.56038/oprd.v4i1.456

c_{s_2}	1250	Ns/m	Second suspension damping coefficient
c_{s_3}	1250	Ns/m	Third suspension damping coefficient
c_{s_4}	1250	Ns/m	Fourth suspension damping coefficient
M	1100	kg	Vehicle mass
I_{x_6}	1850	$kg \cdot m^2$	Vehicle inertia moment
I_{x_7}	550	$kg \cdot m^2$	Vehicle inertia moment
σ_a	7000	-	MR damper parameter
σ_0	1500	-	MR damper parameter
σ_1	3000	-	MR damper parameter
σ_2	300	-	MR damper parameter
σ_b	1250	-	MR damper parameter
a_0	1400	-	MR damper parameter
P	75	-	PID coefficient
D	2	-	PID coefficient
Kd	5	-	FLC coefficient
Kde	14	-	FLC coefficient
Kf	20	-	FLC coefficient
a	1.2	m	Chasis length
b	1.4	m	Chasis length
c	0.5	m	Chasis length
d	1	m	Chasis length